

THE CHEMICAL COMPOSITION OF CO-RICH COMET C/2009 P1 (GARRADD) AT $R_h = 2.4$ and 2.0 AU BEFORE PERIHELION*

L. PAGANINI^{1,4}, M. J. MUMMA¹, G. L. VILLANUEVA^{1,2}, M. A. DISANTI¹, B. P. BONEV^{1,2}, M. LIPPI³, AND H. BOEHNHARDT³

¹ Goddard Center for Astrobiology, NASA GSFC, MS 690, Greenbelt, MD 20771, USA; lucas.paganini@nasa.gov

² Department of Physics, Catholic University of America, Washington, DC 20064, USA

³ Max-Planck-Institut für Sonnensystemforschung, Katlenburg-Lindau, Germany

Received 2012 January 10; accepted 2012 January 31; published 2012 March 1

ABSTRACT

We quantified 10 parent volatiles in comet C/2009 P1 (Garradd) before perihelion, through high-dispersion infrared spectra acquired with CRIRES at ESO's Very Large Telescope on UT 2011 August 7 ($R_h = 2.4$ AU) and September 17–21 ($R_h = 2.0$ AU). On August 7, water was searched for but not detected at an upper limit (3σ) of $2.1 \times 10^{28} \text{ s}^{-1}$, while ethane was detected with a production rate of $6.1 \times 10^{26} \text{ s}^{-1}$. On September 17–21, the mean production rate for water was $8.4 \times 10^{28} \text{ s}^{-1}$, and five trace species (CO, C_2H_6 , CH_4 , HCN, and CH, OH) were securely detected, and (3σ) upper limits were retrieved for NH_3 , C_2H_2 , OCS, and HDO. Given the relatively large heliocentric distance, we explored the effect of water not being fully sublimated within our field of view and identified the “missing” water fraction needed to reconcile the retrieved abundance ratios with the mean values found for “organics-normal” comets. The individual spatial profiles of parent volatiles and the continuum displayed rather asymmetric outgassing. Indications of H_2O and CO gas being released in different directions suggest chemically distinct active vents and/or the possible existence of polar and apolar ice aggregates in the nucleus. The high fractional abundance of CO identifies comet C/2009 P1 as a CO-rich comet.

Key words: astrochemistry – comets: general – comets: individual (C/2009 P1 (Garradd)) – infrared: planetary systems – molecular processes – Oort Cloud

Online-only material: color figures

1. INTRODUCTION

Until 2005, cometary nuclei were thought to be primordial remnants from the giant planets' accretion zone (then viewed as 5–30 AU from the proto-Sun), but subsequent dynamical studies challenge this view and demonstrate the need for an alternative metric of cometary origins (Morbidelli et al. 2008; Levison et al. 2010; Walsh et al. 2011). Those origins are most directly inferred from the properties of native materials (dust, ice) in the nucleus.

Since 1985, measurements of nucleus composition have revealed major diversity among comets, based on crystallinity of silicates and/or the chemistry of native ices. The interpretation, however, is partly linked to questions of orbital evolution. A comet making its first apparition after ejection from the long-term storage reservoir (Kuiper Belt, Oort Cloud) may reveal primordial composition (although cosmic ray processing might affect the properties of the outer layers of cometary nuclei during dynamical storage). Comets in short-period orbits, on the other hand, may have experienced thermo-chemical evolution over successive apparitions that may induce changes from primordial composition. In addition, the number of comets quantified to date in terms of primary (parent) volatiles is still relatively small, restricting full taxonomic classification of origins (for a recent review of cometary taxonomies and natal heritage, see Mumma & Charnley 2011). Here, we present results for the volatile fraction of Oort Cloud (OC) comet C/2009 P1 (Garradd), hereafter C/2009 P1, and discuss them in the context of an emerging cometary taxonomy based on primary volatiles.

C/2009 P1 was discovered at $R_h = 8.7$ AU by G. J. Garradd on UT 2009 August 13, when it displayed a circular (15'' diameter) coma with a visual magnitude ~ 17 . Its orbit is inclined to the ecliptic by 106.2° , and the Tisserand parameter (T_j) and original semi-major axis⁵ are -0.432 and 2564.1 AU, respectively. Together, these classify C/2009 P1 as a nearly isotropic (long period) comet from the OC reservoir.

In this Letter, we present results obtained from near-IR observations of comet C/2009 P1 at the Very Large Telescope (VLT). These results, along with our current characterization of its organic-rich gas production and favorable astrometric positioning, establish C/2009 P1 as a prime target for astronomical observations through early 2012.

2. OBSERVATIONS

We observed comet C/2009 P1 with the Cryogenic high-Resolution InfraRed Echelle Spectrograph (CRIRES) at VLT located in the Atacama desert (Chile), on UT 2011 August 7 and on five consecutive nights spanning September 17–21.⁶ CRIRES provided a spectral resolution ($\lambda/\Delta\lambda$) of about 50,000 using an entrance slit of 0'.4 (in width) and spatial coverage of 40'' (in length) (Käufl et al. 2004). Weather conditions were optimal during our September observations, with low wind speeds of 3 m s^{-1} (5 m s^{-1}), relative humidity of 5% (10%), and water vapor of 1.2 mm (2.1 mm) on the first two nights (remaining nights). Seeing was in the range of 0'.5–0'.9. Standard stars (BS 7235 and BS 7906) located near the comet's trajectory

⁵ S. Nakano Note, NK 2109, <http://www.oaa.gr.jp/~oaaacs/nk/nk2109.htm>

⁶ The core of this Letter is based on the September dates. During the August run, there were difficulties to close AO loop (limiting the sensitivity of our observations). Results from UT 2011 August 7 are presented briefly in Section 3.2, Table 1, and Figure 3.

* Based on observations obtained at the European Southern Observatory at Cerro Paranal, Chile, under program 087.C-0710.

⁴ NASA Postdoctoral Fellow.

Table 1
Molecular Parameters for Primary Volatiles in C/2009 P1 (Garradd)^a

| Species | Time (UT) | T_i^b (minute) | Lines | ν^c (cm ⁻¹) | T_{rot} (K) | GF ^d | Global Q ^e (10 ²⁶ s ⁻¹) | Abundance (%) |
|--|------------|------------------|-------|-----------------------------|----------------------------------|--------------------|---|---------------------------|
| 2011 August 7 ^f $R_h = 2.40$ AU, $\Delta = 1.47$ AU, P.A. = 187°9, $\alpha = 12$:6 | | | | | | | | |
| H ₂ O | 5:15–6:01 | 32 | 9 | 3421.38 | (40) ^g | (1.5) ^h | <208.9 | 100 |
| C ₂ H ₆ | 6:13–7:03 | 32 | 4 | 2986.73 | (40) | (1.5) | 6.1 ± 0.7 | >2.90 |
| 2011 September 17 $R_h = 2.03$ AU, $\Delta = 1.55$ AU, P.A. = 98°0, $\alpha = 28$:7 | | | | | | | | |
| H ₂ O | 0:25–1:15 | 40 | 7 | 3397.19 | (50) ⁱ | 1.8 | 841.8 ± 64.2 | 100 |
| C ₂ H ₆ | 1:24–2:50 | 52 | 4 | 2988.42 | 49 ⁺²⁹ ₋₁₃ | 1.4 | 8.8 ± 0.7 | 1.04 ± 0.11 |
| CH ₄ | " | " | 2 | 3033.63 | (50) | 1.4 | 11.3 ± 1.5 | 1.34 ± 0.21 |
| 2011 September 18 $R_h = 2.02$ AU, $\Delta = 1.55$ AU, P.A. = 97°0, $\alpha = 29$:0 | | | | | | | | |
| H ₂ O | 23:56–1:06 | 48 | 2 | 2148.01 | (50) | 1.4 | 833.1 ± 147.8 | 100 |
| CO | " | " | 8 | 2152.97 | 51 ± 2 | 1.4 | 113.2 ± 8.6 | 13.45 ± 1.45 ^j |
| HCN | 1:20–2:38 | 64 | 8 | 3310.38 | 52 ⁺⁹ ₋₈ | 1.5 | 2.9 ± 0.3 | 0.35 ± 0.04 ^j |
| C ₂ H ₂ | " | " | 9 | 3296.45 | (50) | (1.5) | <1.1 | <0.13 ^j |
| NH ₃ | " | " | 6 | 3320.77 | (50) | (1.5) | <14.2 | <1.69 ^j |
| 2011 September 19 $R_h = 2.02$ AU; $\Delta = 1.56$ AU, P.A. = 96°0, $\alpha = 29$:3 | | | | | | | | |
| H ₂ O | 0:22–1:15 | 40 | 1 | 2039.96 | (50) | (1.5) | 883.3 ± 306.6 | 100 |
| OCS | " | " | 7 | 2057.61 | (50) | (1.5) | <1.6 | <0.20 ^j |
| HDO | 1:26–2:22 | 40 | 9 | 2684.78 | (50) | (1.5) | <7.5 | <0.89 ^{j,k} |
| 2011 September 20 $R_h = 2.01$ AU; $\Delta = 1.57$ AU, P.A. = 95°1, $\alpha = 29$:5 | | | | | | | | |
| H ₂ O ^l | 23:41–1:07 | 60 | 6 | 3306.7 | (50) | (1.5) | 838.7 ± 170.2 | 100 |
| HCN | " | " | 7 | 3305.75 | 47 ± 6 | 1.5 | 3.1 ± 0.3 | 0.37 ± 0.05 ^m |
| C ₂ H ₂ | " | " | 8 | 3288.90 | (50) | (1.5) | <1.2 | <0.14 ^m |
| NH ₃ | " | " | 6 | 3328.25 | (50) | (1.5) | <11.8 | <1.40 ^m |
| CH ₃ OH | 1:15–2:33 | 56 | 9 | 2837.52 | 48 ⁺¹⁰ ₋₆ | 1.7 | 32.8 ± 3.7 | 3.90 ± 0.53 ^m |
| 2011 September 21 $R_h = 2.00$ AU; $\Delta = 1.58$ AU, P.A. = 94°2, $\alpha = 29$:8 | | | | | | | | |
| H ₂ O | 23:50–0:44 | 42 | 11 | 3403.40 | 51 ⁺²⁴ ₋₁₉ | 1.5 | 840.5 ± 66.9 | 100 |
| CO | 0:51–1:32 | 32 | 8 | 2152.97 | 60 ± 5 | 1.7 | 97.2 ± 6.7 | 11.56 ± 1.19 |
| C ₂ H ₆ | 2:02–2:34 | 24 | 4 | 2988.42 | 48 ⁺²⁵ ₋₁₅ | 1.4 | 8.2 ± 0.7 | 0.98 ± 0.11 |
| CH ₄ | " | " | 2 | 3033.63 | (50) | 1.4 | 9.6 ± 2.6 | 1.14 ± 0.33 |

Notes.

^a Mixing ratios (in percent) are expressed relative to H₂O. Uncertainties represent 1 σ , and upper limits represent 3 σ . The reported error in production rate includes the line-by-line scatter in measured column densities, along with photon noise, systematic uncertainty in the removal of the cometary continuum, and (minor) uncertainty in rotational temperature. (For further details, please contact the corresponding author.)

^b Total on-source integration time.

^c Mean frequency of all emission lines (used for this reduction) from a particular species.

^d Growth factor.

^e Global production rate, after applying a measured growth factor (and its error of ± 0.1) to the nucleus-centered (NC) production rate.

^f R_h : heliocentric distance; Δ : geocentric distance; P.A.: position angle of the extended Sun–comet vector; α : Solar Phase (Sun–comet–Earth) angle, see upper-right compass in Figure 4. (These values represent the mid point of data acquisition.)

^g Assumed rotational temperature based on September observations.

^h For molecules whose growth factor is not measured directly, we adopt GF = (1.5).

ⁱ We tabulate the retrieved T_{rot} and confidence limits. Measured temperatures are consistent with 53 K for all molecules. We adopted $T_{rot} = 50$ K when calculating the NC production rates for all species whose T_{rot} determination was not possible. This is indicated as (50).

^j The stated molecular abundance ratios use the water production rate from September 17.

^k D/H in water <29 VSMOW (3 σ).

^l Retrieval of the water production rate is based on OH* emission lines, a direct proxy for water (Boney et al. 2006).

^m The stated molecular abundance ratios use the water production rate from September 21.

allowed flux calibration and measures of column burdens for absorbing species in the terrestrial atmosphere. The CRILES entrance slit (0'.4 × 40'') was positioned along the projected Sun–comet direction on all five nights. The observing log is given in Table 1.

Cometary spectra were acquired in a four-step sequence (ABBA) with an integration time of 60 s (or 120 s) per step, nodding the telescope along the slit by 11'' between the A and B positions. We followed our standard procedures for initial data reduction and analysis of the individual echelle orders (DiSanti et al. 2001; Villanueva et al. 2011a), which included flat fielding, removal of high dark current pixels and cosmic-ray hits, spatial

and spectral rectification, and spatial registration of individual A and B beams. After combining the A and B beams from the difference frames, we extracted a spectrum from the sum of 15 spatial rows (1''/29) centered on the nucleus (this also assists in removing the residual background).

The simultaneous measurement of H₂O or its direct proxy (OH*) in each instrument setting permitted accurate characterization of the abundance ratio for each trace species. Six primary volatiles (H₂O, CO, C₂H₆, CH₄, HCN, and CH₃OH) were securely detected, and upper limits were retrieved for NH₃, C₂H₂, OCS, and HDO. As mentioned in our IAU Circular (Paganini et al. 2011) and shown in Figure 1, detections of eight

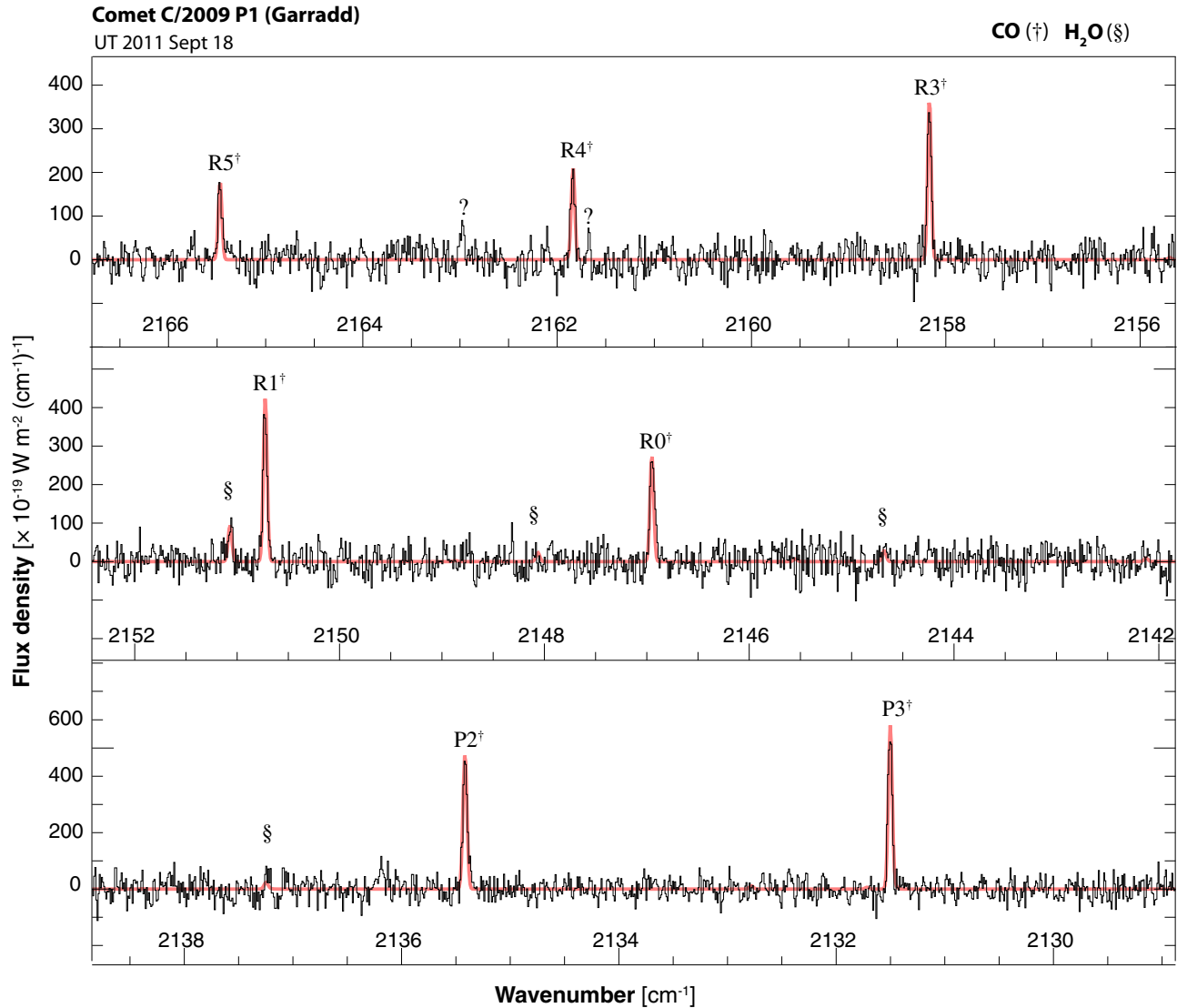


Figure 1. Emission spectra of C/2009 P1 near $4.7 \mu\text{m}$. Rovibrational lines of the CO fundamental band ($v = 1-0$) and H₂O (hot bands) are apparent. The CO analysis was based on the CO R6–P3 lines shown here, along with the R7 line (not shown). Here, and in Figure 2, the continuous (underlying) red line depicts the modeled spectra. Also, several unidentified lines are indicated (?).

(A color version of this figure is available in the online journal.)

prominent CO emission lines enabled robust retrieval of a (high) CO/H₂O ratio. Detections of other primary volatiles are shown in Figure 2. Several unidentified lines are seen in these spectra; however, we defer a complete analysis to a future publication. Figure 3 shows the temporal development of specific production rates. Figure 4 displays spatial profiles for six volatiles, the cometary continuum, and the flux standard star for all days. On the third night (September 19), we emphasized OCS and HDO but obtained only upper limits, and a retrieval of spatial profiles was not possible.

3. RESULTS AND DISCUSSION

Comet C/2009 P1 displayed significant outgassing at these pre-perihelion positions ($R_h = 2.4$ and 2.0 AU). Specific results are shown in Table 1 for each setting, date, and volatile species. In the following subsections we highlight our major findings.

3.1. Rotational Temperatures

We retrieved accurate rotational temperatures for H₂O, CO, C₂H₆, HCN, and CH₃OH by performing excitation analyses

of extracted and predicted intensities for spectral lines of a given molecule. Predicted intensities were obtained from our custom fluorescence models (Villanueva et al. 2011a, 2011b, and references therein). A rotational temperature of 50 K is consistent with the average temperature from these five volatiles, although some minor differences are observed (Table 1).

3.2. Production Rates and Abundance Ratios

Production rates of H₂O and HCN displayed rather stable outgassing during the five nights in September, as opposed to C₂H₆, CO, and CH₄ whose relative production decreased by $\sim 15\%$ from September 18–19 to 21. During this interval, H₂O and HCN changed by less than 5% (see Figure 3). The mean production rates (over the entire observing interval) for each volatile species are: H₂O ($8.4 \times 10^{28} \text{ s}^{-1}$), CO ($1.1 \times 10^{28} \text{ s}^{-1}$), CH₃OH ($3.3 \times 10^{27} \text{ s}^{-1}$), CH₄ ($1.0 \times 10^{27} \text{ s}^{-1}$), C₂H₆ ($8.5 \times 10^{26} \text{ s}^{-1}$), and HCN ($3.0 \times 10^{26} \text{ s}^{-1}$). Abundances relative to water are: CO (12.51%), CH₃OH (3.90%), CH₄ (1.24%), C₂H₆ (1.01%), and HCN (0.36%). Upper limits (3σ) were obtained

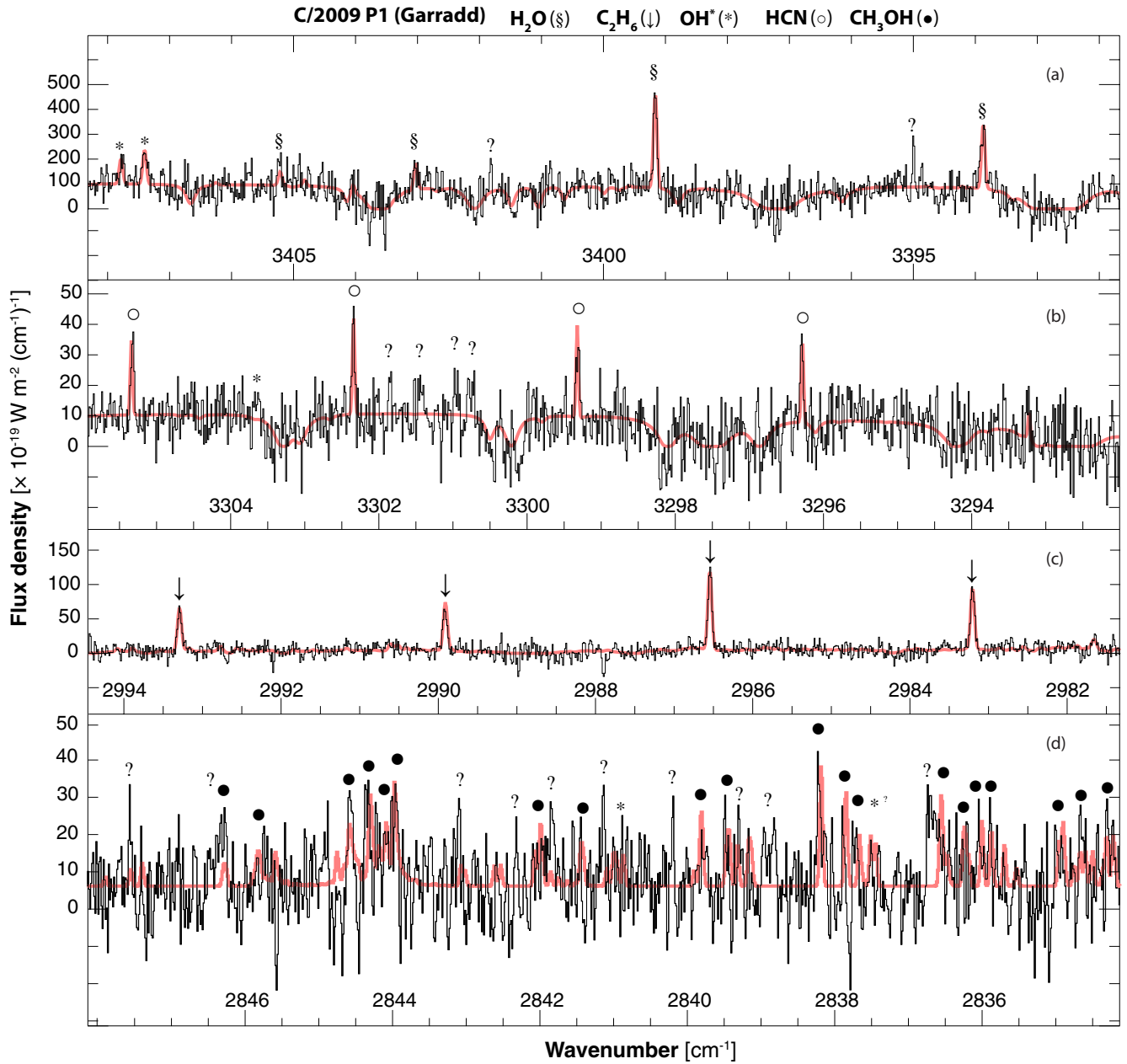


Figure 2. Detections of four primary volatiles and OH prompt emission (a direct proxy for water) in comet C/2009 P1 (Garradd). The continuum from cometary dust is detected. (a) H₂O and OH* lines detected on UT 2011 September 17. (b) HCN lines detected on UT 2011 September 18. (c) Ethane ν_7 Q-branches detected on UT 2011 September 17. (d) Methanol emission lines (ν_3 -band) detected on UT 2011 September 20. Several unidentified lines are indicated (?).

(A color version of this figure is available in the online journal.)

for the abundance ratio for four minor species: NH₃ (<1.55%), C₂H₂ (<0.13%), HDO (<0.89%), and OCS (<0.20%).

On 2011 August 7 ($R_h = 2.4$ AU), water was searched but not detected at an upper limit (3σ) of 2.1×10^{28} s⁻¹, while ethane was detected with a production rate of 6.1×10^{26} s⁻¹. When compared with measurements of C₂H₆ in mid-September, the production of ethane in August is consistent with insolation-limited outgassing (varying as $R_h^{-2.2}$). The upper limit for water suggests a mixing ratio for ethane >2.90% (3σ), which far exceeds the abundance ratio measured in late September. The likely explanation is that water sublimation was less fully activated at 2.4 AU, compared with 2.0 AU.

D. Schleicher (2011, private communication) reports water production rates at (R_h) 2.49 AU (July 28) and 1.97 AU

(September 24) that are larger than our values on nearby dates. If we adjust the sublimated water fraction in mid-September to achieve “normal” abundances of C₂H₆ ($\sim 0.52\%$) and/or HCN ($\sim 0.23\%$), the water production rate would increase by about 60%–90%, resulting in abundance ratios of CO $\sim 7.26\%$, C₂H₆ $\sim 0.59\%$, CH₄ $\sim 0.72\%$, HCN $\sim 0.21\%$, and CH₃OH $\sim 2.26\%$. If the “missing” fraction were pure water ice, this increase would reconcile water production rates estimated in the infrared to those obtained in the optical. An even larger “missing” fraction is required at 2.4 AU. *AKARI* observed an increase in mixing ratios for CO₂ beyond 2.5 AU (Ootsubo et al. 2011), demonstrating the decreasing efficiency of water ice sublimation at heliocentric distances beyond 2.5 AU.

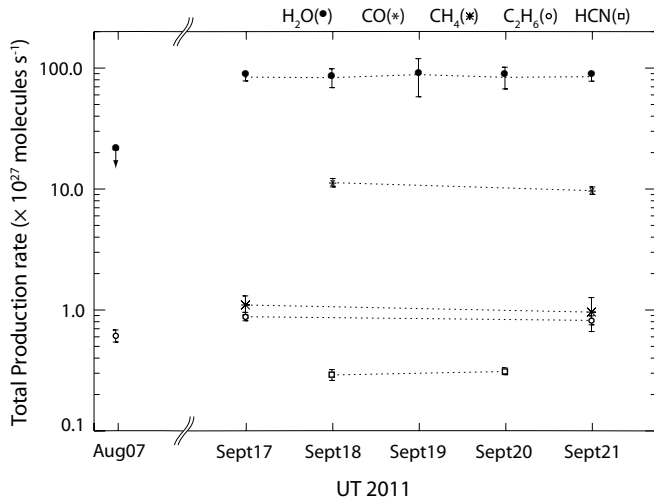


Figure 3. Evolution of total production rates during our observing campaign.

3.3. Spatial Profiles

During our September observations, we oriented the slit along the extended comet–Sun projected radius vector (Position Angle, P.A., $\sim 96^\circ$). The solar phase angle of 29.5° (Table 1) indicates that the sub-solar point was well placed within the nucleus hemisphere seen from the Earth.

During the first night (UT 2011 September 17; see Figure 4(a)), the (asymmetric) water profile displayed strong enhancement in the sunward direction (here, we use “sunward” to mean the directed projection on the sky plane of the comet–Sun vector). The profile of ethane was also enhanced in the sunward direction, but less so than that of water. The methane profile was symmetric about the nucleus and displayed a steep slope in both directions with a secondary minimum at ~ 2000 km sunward.

On the second night (UT 2011 September 18, see Figure 4(b)), CO and HCN showed profiles that were somewhat enhanced in the anti-sunward direction. HCN displayed a secondary minimum at 2000 km sunward, similar to CH_4 on the previous

night. Likewise, the profile of OH^* (a direct tracer of H_2O) showed a behavior similar to that of water on the previous night.

Compared to the continuum, CH_3OH showed some enhancement on both sides during the fourth night (UT 2011 September 20; see Figure 4(c)); meanwhile, HCN displayed flux excess toward negative pixels only (to the left in Figure 4(c)). HCN displayed a broader profile than that seen on September 18, perhaps suggesting enhanced gas release on September 20. (A profile for H_2O or OH^* was not possible during this night due to the low signal-to-noise ratio of these lines.)

On the fifth night (UT 2011 September 21; see Figure 4(d)), water showed behavior similar to the first and second nights (i.e., some flux increase toward positive pixels). Ethane displayed a less asymmetric profile, compared with the first night, with minor flux excess in the anti-sunward direction. CO followed the continuum profile in the sunward direction, as opposed to the anti-sunward side, where its flux was clearly enhanced compared to the continuum (somewhat similar to HCN and CH_3OH on the previous night).

The continuum profile displayed higher intensity toward the sunward direction on all nights (slope differences in the anti- and sunward directions are confirmed by log–log representations of the flux profile along the slit). These molecules displayed distinctive schemes of gas release, although some particular structures are found. Compared to the continuum profile, we note that water (and OH^*) is clearly enhanced in the sunward side on three nights (1, 2, and 5), similar to methanol on the fourth night. Conversely, spatial profiles of CO, HCN, and (also) CH_3OH displayed flux excess in the anti-sunward direction; meanwhile C_2H_6 and CH_4 showed similar (rather symmetric) profiles. These configurations strengthen the idea of separate polar (H_2O -rich) and apolar (CO-rich) ice aggregates whose accreting gas composition underwent different chemical processes before incorporation in the nucleus, or re-distribution after incorporation.

The flux excess seen relative to the continuum for some volatiles (especially H_2O , CO, and methanol) suggests the presence of a delayed sublimation mechanism, such as icy grains sublimating in the coma. The spatial profiles of some volatiles

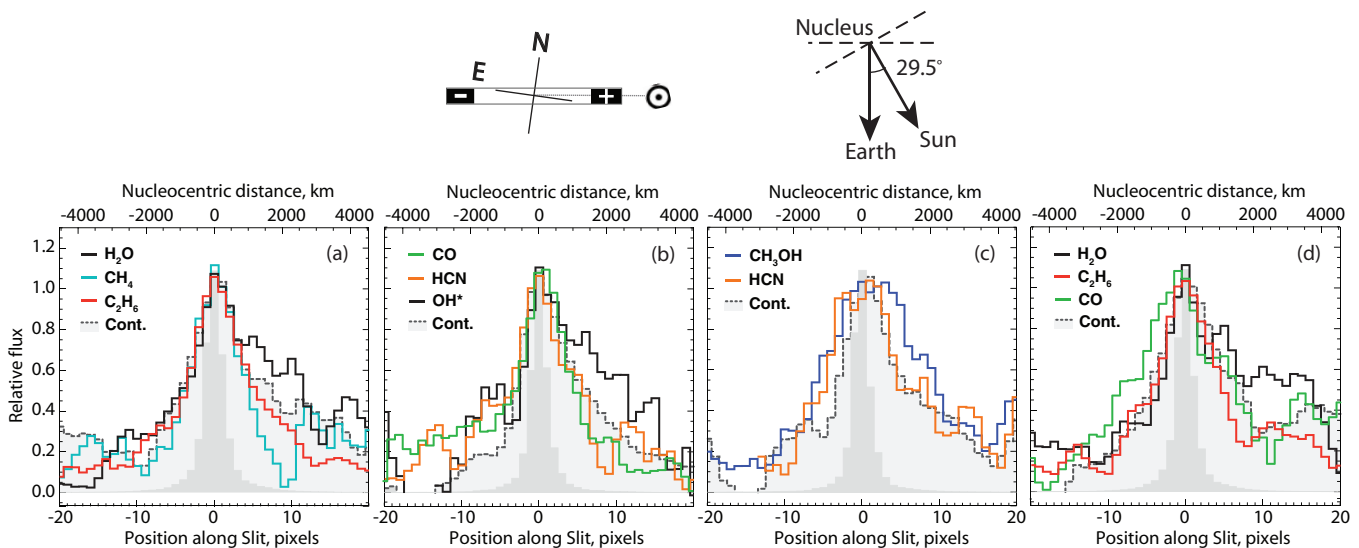


Figure 4. Spatial profiles of primary volatiles and continuum in comet C/2009 P1 on four nights: (a) UT 2011 September 17, (b) September 18, (c) September 20, and (d) September 21. The slit was positioned along the projected comet–Sun radius vector (P.A. $\sim 96^\circ$), and the projected sunward direction (+) and solar phase angle (29.5°) are marked. The measured stellar point-spread function and continuum are shaded (dark gray and light gray, respectively). Profiles are discussed in Section 3.3. (A color version of this figure is available in the online journal.)

display regular patterns, with a separation of ~ 1000 – 1500 km between peaks (see Figure 4). These patterns are also present in observations of water emission lines with NIRSPEC in 2011 October (M. A. DiSanti et al. 2012, in preparation). On the other hand, active regions producing directed outflow with heterogeneous composition and different rotational phases could also produce such behavior, without a delayed sublimation mechanism. We are not able to rule out either possibility with the evidence in hand.

3.4. The (Relatively) High Abundance of CO

Measurements of cometary composition suggest rather low (or depleted) carbon monoxide relative to H_2O in most comets (Bockelée-Morvan et al. 2004; Mumma & Charnley 2011). The measured abundance ratios (from ground-based studies) range from 0.2% to $\sim 24\%$, but only four comets displayed $\text{CO} > 10\%$, relative to water. A recent survey of 18 comets (10 JFCs and 8 OC comets) at heliocentric distances between 1 and 4 AU by the AKARI mission (Ootsubo et al. 2011) found a similar paucity of comets enriched in CO. Comets within 2.5 AU of the Sun revealed little (or no) CO content (mostly upper limits were retrieved), though their CO_2 abundance varied from a few to $\sim 30\%$ (relative to water). An exception was comet C/2008 Q3 (Garradd) that displayed $\text{CO}/\text{H}_2\text{O} \sim 30\%$ (at $R_h = 1.7$ AU). Abundance ratios of CO and CO_2 in comets surveyed beyond ~ 2.5 AU were likely “artificially” enhanced by the increasing stability (against sublimation) of water ice.

Valuable lessons are also taken from observations toward young stellar objects (YSOs). Ices control much of the star formation process and account for most oxygen and carbon in a protostellar environment (Öberg et al. 2011), so comparing these abundances to those found in comets provides useful tests of the possible influence of thermal (and chemical) processing of cometary material before accretion. Measurements in Galactic YSOs have resulted in $\text{CO}/\text{H}_2\text{O}$ in the range of 2%–20% (Chiar et al. 1998; Gibb et al. 2004) and $\text{CO}_2/\text{H}_2\text{O}$ in the range of 10%–23% (Gerakines et al. 1999), which may indicate high ratios $\text{CO}_2/\text{H}_2\text{O}$ rather than depleted carbon monoxide in comets.

On the other hand, comets such as C/1995 O1 (DiSanti et al. 1999, 2001), C/1996 B2 (Mumma et al. 1996; Biver et al. 1999; DiSanti et al. 2003), C/1999 T1 (Mumma et al. 2003), C/2008 Q3 (Ootsubo et al. 2011), and C/2009 P1 (this work), revealed high abundances of CO relative to H_2O , and thus these “peculiar” exceptions (compared to the normal trend) are not trivial. Owing to its desorption temperature (15–30 K, depending on the ice mixture), CO ice is strongly susceptible to the effect of thermal processing by stellar radiation. A study by Shimonishi et al. (2010) confirmed the systematic difference in the CO ice abundance of luminous YSOs in the Large Magellanic Cloud (LMC), demonstrating the key influence of stellar radiation on CO ice abundance (unlike CO_2 ice).

Even though H_2O , CO, and CO_2 are the most abundant ices in molecular clouds before the onset of collapse, their formation chemistry and content in comets are still poorly understood. Simulations of the chemical evolution considering the effect of turbulent transport of gases and ices in planetary disks have proven to be useful for understanding the measured abundances of these ices in comets (e.g., Semenov & Wiebe 2011). These results, along with observational evidence of clear diversity in the chemical composition of comets, demonstrate the importance of radial mixing and transport from different regions into the comet’s formative zone (putatively, $R_h = 5$ – 30 AU), probably at different evolutionary stages of the young proto-Sun. Indeed, the

long-held hypothesis relating crystallinity in cometary silicates to high-temperature processing of pre-cometary grains was recently confirmed by detailed laboratory investigations of rocky samples returned from 81P/Wild 2 by *Stardust* (Brownlee et al. 2006). Formed within 10 solar radii, these refractory silicates were carried outward to the region where even hypervolatile gases could condense, sheathing them in ices of water and organic volatiles. Successive aggregation later formed ever-larger bodies, culminating in the final icy planetesimal now known as the nucleus of comet Wild 2.

The possible connection between interstellar chemistry and cometary ices has been greatly strengthened by observations of several bright comets, especially C/1995 O1 (Hale-Bopp) (e.g., Ehrenfreund et al. 1997; Bockelée-Morvan et al. 2000). As Mumma & Charnley (2011) discussed in their review, planetesimals in cometary nuclei stem from interstellar matter that underwent different degrees of chemical and dynamical processing before aggregation. Thus, considering the formation of cometary nuclei from material with distinct chemical histories, i.e., various degrees of processing (including pristine material, cf. Visser et al. 2011), the high CO composition found in comet C/2009 P1 (and in other similar CO-rich comets) strengthens the idea that some material formed in outer regions in the disk, where stellar radiation was less intense and so CO was better shielded from external catalysts. Other possible scenarios include the possible capture of CO within the water ice mantles, which would produce desorption only at higher temperature. Perhaps the most extreme issue is the possible capture of these comets from stars in the Sun’s birth cluster (Levison et al. 2010).

4. CONCLUSIONS

Among the organic compounds measured, we find a relative enhancement of organic volatiles in C/2009 P1 (Garradd), compared to other OC comets in our IR survey. CO is significantly enhanced, CH_4 is toward the high end of values found to date, CH_3OH is somewhat enhanced, and C_2H_6 and HCN are normal to slightly enhanced. Our abundance of CH_4 and HCN were similar to values found in other CO-rich comets (excepting C/1996 B2, which had a lower amount of CH_4), while CH_3OH and C_2H_6 have similar to enhanced abundances among these comets.

In this work, we presented abundance ratios (in percent) relative to water. If we consider the possible effect of water not being fully sublimated within our field of view (FOV) at the observed heliocentric distance (~ 2 AU), and adjust the water fraction to achieve “normal” abundances of C_2H_6 and HCN, the water production rate would increase by $\sim 60\%$ – 90% . Our non-detection of water in 2011 August could be related to this effect. If this added fraction were pure water ice, its addition would bring the abundance ratios of most other minor species (i.e., C_2H_6 , CH_4 , CH_3OH , and HCN) in agreement with values in the “organics-normal” group (Mumma et al. 2003; Bockelée-Morvan et al. 2004; DiSanti & Mumma 2008). However, the CO abundance would decrease to about 7.26%, which is still higher than that seen in most OC comets. Possible explanations for a high CO composition suggest accretion in the outer region of the protoplanetary disk that underwent minor (if any) thermal processing before incorporation into the nucleus. Upcoming measurements at smaller heliocentric distances will provide additional tests of this issue.

We thank ESO’s VLT team. L.P. thanks the NASA Postdoctoral Program. M.J.M., G.L.V., and M.A.D. acknowledge NASA’s Astrobiology, PAST, and PATM. B.P.B. acknowledges

NSF. H.B. and M.L. acknowledge support from IMPRS and GIF.

REFERENCES

- Biver, N., Bockelée-Morvan, D., Crovisier, J., et al. 1999, *AJ*, **118**, 1850
- Bockelée-Morvan, D., Crovisier, J., Mumma, M. J., & Weaver, H.A. 2004, in *Comets II*, ed. M. C. Festou, H. U. Keller, & H. A. Weaver (Tucson, AZ: Univ. Arizona Press), 391
- Bockelée-Morvan, D., Lis, D. C., Wink, J. E., et al. 2000, *A&A*, **353**, 1101
- Bonev, B. P., Mumma, M. J., DiSanti, M. A., et al. 2006, *ApJ*, **653**, 774
- Brownlee, D. E., Tsou, P., Aléon, J., et al. 2006, *Science*, **314**, 1711
- Chiar, J. E., Gerakines, P. A., Whittet, D. C. B., et al. 1998, *ApJ*, **498**, 716
- DiSanti, M. A., & Mumma, M. J. 2008, *Space Sci. Rev.*, **138**, 127
- DiSanti, M. A., Mumma, M. J., Dello Russo, N., & Magee-Sauer, K. 2001, *Icarus*, **153**, 361
- DiSanti, M. A., Mumma, M. J., Dello Russo, N., Magee-Sauer, K., & Griep, D. M. 2003, *J. Geophys. Res.*, **108**, 5061
- DiSanti, M. A., Mumma, M. J., Dello Russo, N., et al. 1999, *Nature*, **399**, 662
- Ehrenfreund, P., D'Hendecourt, L., Dartois, E., et al. 1997, *Icarus*, **130**, 1
- Käufel, H., Ballester, P., Biereichel, P., et al. 2004, *Proc. SPIE*, **5492**, 1218
- Gerakines, P. A., Whittet, D. C. B., Ehrenfreund, P., et al. 1999, *ApJ*, **522**, 357
- Gibb, E. L., Whittet, D. C. B., Boogert, A. C. A., & Tielens, A. G. G. M. 2004, *ApJS*, **151**, 35
- Levison, H. F., Duncan, M. J., Brasser, R., & Kaufmann, D. E. 2010, *Science*, **329**, 187
- Morbidelli, A., Levison, H. F., & Gomes, R. 2008, in *The Solar System Beyond Neptune*, ed. M. A. Barucci et al. (Tucson, AZ: Univ. Arizona Press), 275
- Mumma, M. J., & Charnley, S.B. 2011, *Ann. Rev. Astron. Astrophys.*, **49**, 471
- Mumma, M. J., DiSanti, M. A., Dello Russo, N., et al. 1996, *Science*, **272**, 1310
- Mumma, M. J., DiSanti, M. A., Dello Russo, N., et al. 2003, *Adv. Space Res.*, **31**, 2563
- Öberg, K. I., Boogert, A. C. A., Pontoppidan, K. M., et al. 2011, *ApJ*, **740**, 109
- Ootsubo, T., Kawakita, H., Hamada, S., et al. 2011, EPSC-DPS Joint Meeting 2011, Vol. 6, *EPSC-DPS2011-369*
- Paganini, L., Mumma, M. J., Lippi, M., et al. 2011, *IAU Circ.*, **9238**, 2
- Semenov, D., & Wiebe, D. 2011, *ApJS*, **196**, 25
- Shimonishi, T., Onaka, T., Kato, D., et al. 2010, *A&A*, **514**, 12
- Villanueva, G. L., Mumma, M. J., DiSanti, M.A., et al. 2011a, *Icarus*, **216**, 227
- Villanueva, G. L., Mumma, M. J., & Magee-Sauer, K. 2011b, *J. Geophys. Res.*, **116**, 1
- Visser, R., Doty, S. D., & van Dishoeck, E. F. 2011, *A&A*, **534**, A132
- Walsh, K. J., Morbidelli, A., Raymond, S. N., O'Brien, D. P., & Mandell, A. M. 2011, *Nature*, **475**, 206

ERRATUM: “THE CHEMICAL COMPOSITION OF CO-RICH COMET C/2009 P1 (GARRADD)
AT $R_h = 2.4$ AND 2.0 AU BEFORE PERIHELION” (2012, *ApJ*, 748, L13)

L. PAGANINI^{1,4}, M. J. MUMMA¹, G. L. VILLANUEVA^{1,2}, M. A. DISANTI¹, B. P. BONEV^{1,2}, M. LIPPI³, AND H. BOEHNHARDT³

¹Goddard Center for Astrobiology, NASA GSFC, MS 690, Greenbelt, MD 20771, USA; lucas.paganini@nasa.gov

²Department of Physics, Catholic University of America, Washington, DC 20064, USA

³Max-Planck-Institut für Sonnensystemforschung, Katlenburg-Lindau, Germany

Received 2012 August 16; published 2012 August 24

Due to an error at the publisher, the third sentence of the abstract of the published version of this article contains a mistake. The corrected version should be:

On September 17–21, the mean production rate for water was $8.4 \times 10^{28} \text{ s}^{-1}$, and five trace species (CO, C₂H₆, CH₄, HCN, and CH₃OH) were securely detected, and (3σ) upper limits were retrieved for NH₃, C₂H₂, OCS, and HDO.

IOP Publishing sincerely regrets this error.

⁴ NASA Postdoctoral Fellow